Understanding Pressure Compartmentalization in Ultra-Deepwater Drilling Off Mexican Gulf Coast: A Case Study*

Leonardo Enrique Aguilera Gomez[1], Francisco Espitia Hernandez[1], Devendra Kumar[2], Chandramani Shrivastava[3], Javier Contreras Trejo[1], Enrique Guzman Vera[1], Eduardo Roman Garcia[1], Pierre Bonningue[2], Joseph Gremillion[2], Yacira Hamana[2], Enrique Montes Carrasco[2], Constancio Barajas Gea[2], Hector Alonso[2], Monserrat Vera[2], and Claudia Romero[2]

Search and Discovery Article #41361 (2014)
Posted May 30, 2014

*Adapted from extended abstract prepared in conjunction with poster presentation at AAPG 2014 Annual Convention and Exhibition, Houston, Texas, April 6-9, 2014, AAPG © 2014

[1]Pemex, Ciudad Del Carmen, Campeche, Mexico
[2]PTS, Schlumberger, Ciudad Del Carmen, Campeche, Mexico (DKumar6@slb.com)
[3]Wireline, Schlumberger, Lagos, Nigeria

Abstract

Presure compartmentalization while drilling a well poses a lot of challenges, if not accounted for with the help of accurately built models which are continuously updated with data acquisition during the drilling. The southern Gulf of Mexico has witnessed a lot of ultra-deepwater drilling activity in recent times, and it is imperative to understand the pressure-compartmentalization through drilled section for better evaluation of reservoirs, in addition to the informed-drilling in the next wells in this setting.

Pressure data acquired in the study area suggests that formations above Miocene are hydrostatic in nature and pressure gradually increases in middle Miocene where pressure gradient has been observed to build up to 0.63psi/ft. Drilling challenges arise while entering lower Miocene where a steep pressure ramp of over 3psi/ft has been encountered.

Pressure compartmentalization of this order is critical to understand, not only for optimal drilling but also to understand the subsurface complexities for formation evaluation. In this study, a multi-disciplinary approach is used to understand and identify

the pressure seals and associated variations in well-log measurements. Regional geological setting was studied with well-centric borehole images to establish the local geological variations in the study area. Petrophysical well logs were studied for clay-typing in different wells to assess the possibility of clay transformation to the overpressured zones. Acoustic anisotropy measurements and stress analysis were compared against the pressure profiles to understand the distribution of overpressured zones and their impact on the wells. Background shale pressure was compared with the measured pressure in sands to understand the sand-shale equilibrium; in conjunction with petrophysical analysis of lower and middle Miocene formations to delineate the pressure transition. While exiting Miocene and entering Oligocene formations, pressure gradient reduces to ~0.8psi/ft.

This case study discusses the response of various measurements to observed pressure compartmentalization in study wells and seeks to establish an understanding in the study area. This also offers a better understanding of the expected subsurface behavior for future drilling, leading to successful exploration in overpressured Tertiary formations in southern part of Mexican Gulf Coast.

Introduction

Post-well analysis of the previously drilled well shows pressure compartments and often causes drilling problems hindering operations (drilling). In general, a simple geopressure model without pressure compartments has been proposed for a well, which has been modified/updated during drilling, more specifically while passing through the Tertiary targets in the study area. Pressure profile and petrophysical interpretation with respect to the geological evolution of the study area helped in understanding the subsurface overpressure regimes, while suggesting possible mechanism for their development and to better prepare for further drilling and evaluation in the region.

While it is possible to see compartmentalization clearly on complete data sets, including while drilling, mud log and wireline data; what is needed is a solution while drilling to identify changes in pressure regimes in time to affect changes to the mud weight and prevent lost time. Due to sensor offset from the bit, pre-drill geopressure model is used as a guide to predict ahead of bit. The model is updated and calibrated with newly acquired logs, pressure measurements and pressure-related events (such as fluid influx, lost circulation, leak-off test, etc.), after every section. The basic workflow used in deepwater is to use real-time density, resistivity and sonic compressional slowness data to estimate pore pressure in real-time. Using both simple trend line analysis and effective stress to calculate several different estimates of pore pressure that are at different measurement points and distances from the bit. The problem occurs when a new pressure compartment is entered, and the previous trend line is no longer

valid. By reviewing the 1-d models and trend-line analysis and comparing it to the available petrophysical analysis, the sealing formation could be identified. By identifying the sealing formation, using the log correlation and the characteristic response of the well logs, it is possible to identify the top of a new compartment in real time, and start a new trend-line analysis to accurately estimate pore pressure while drilling.

Background Geology

The study area lies in the southwestern part of Gulf of Mexico, off Mexican coast (Figure 1). The subsurface geology of the study area in the southern Gulf of Mexico, off Mexican coast, is controlled by the complex interplay of Mexican Ridge (Cordilleras Mexicanas, CM) province and Catemaco Foldbelt (Cinturón Plegado de Catemaco, CPC) structures and the deepwater depositional environment. The folding episodes seems to have given rise to a regional unconformity between middle and lower Miocene; providing a regional pressure barrier.

However, depending on the well location, this unconformity might simply grade into conformity elsewhere, as it has been a tectonically active regime where positive relief has not been extensive throughout. Other than the structure-controlled pressure barriers, facies variations also gives rise to some pressure barriers; which might or might not get resolved during the real-time data analysis while drilling. Four study wells are shown with their locations with respect to the structural provinces (CM and CPC). Different sand targets in the study area comprise Tertiary deepwater prospects, Paleocene to Miocene, deposited by submarine channels / fans and turbidites (Figure 2).

Pressure Compartments

Mechanisms responsible for the generation of overpressure require the existence of barriers to retard the fluid flow, but very few of them require the existence of a closed, pressure-sealed compartment. Buoyancy, non-equilibrium flow, irregularities in potentiometric surfaces, and removal of subsurface fluids, only require confined systems. The level of barrier effectiveness required to generate abnormal pressure due to non-equilibrium compaction is highly relative and probably highly variable. Pressure anomalies related to small, temperature- dependent changes in pore-fluid volume (i.e., aquathermal pressuring, smectite to illite transformation, uplift and/or erosion) require the existence of seals and cannot develop as a result of low hydraulic conductivity of enveloping rocks. Therefore, because many mechanisms that generate anomalous pressure do not require seals, the common occurrence of anomalous pressure, without knowledge of timing and mechanism of formation, does not contribute

to answering the question of whether or not seals exist. On the contrary, the seals are not always and/or everywhere required to develop anomalous pressure.

Geopressures in well-A show were almost hydrostatic down to middle Miocene formations, and maximum 1.08g/cc was measured in sand zones, whereas increasing pore pressure trend was observed as soon as lower Miocene formations were encountered. Although sonic data works reasonably well in the region, where calculated pore pressure is a good match with measured pressure data points, resistivity data is often affected (perhaps salinity or lithology), and several deviations from single normal compaction trends can be observed. In such situation, it is required to change the compaction trend line to calibrate the pore pressure (Figure 3). Lower Miocene formation was drilled further without any drilling complications.

Measured pressure data in lower Miocene was full of surprises, where pressure was more than the mud density used to drill the section. Apart from this, normal compaction trend, which was well calibrated down to middle Miocene formation underestimated the pressures (Figure 4). This generated a need to re-investigate and revise the model for upcoming wells. Next well-B was also designed to explore the same formations, and data collected in well-A was used as a guide for geopressure modeling. The pressure ramp which was associated with the formation boundary between middle Miocene and lower Miocene was not observed in this well. The ramp was found far below, in lower Miocene (Figure 5); thereby, implying the limit of seal between the well-A and well-B. It is very important to understand the distribution of depositional facies in environments where intense structural control (folding and faulting) is exercised on deepwater deposits, resulting in irregular seals and pressure barriers. The study area is part of a very complex structural setting, and some formations appear to have been eroded during uplift due to folding, giving rise to unconformity (and missing sections between the wells).

All these uncertainties in the geopressure suggested a need for re-analysis of the data to understand the cause of overpressure. Geopressures can only be accurately measured in the formations with fair porosity and permeability, as it depends upon fluids being able to flow from the formation into the probing device. Hence, pressure can only be measured in reservoir-type rocks and cannot be measured in potential seals. Conversely, geopressure can be modeled in low-permeability formations, potential sealing rocks, such as shales. To reduce complexities in modeling, it has often been assumed (perhaps incorrectly) that the pressure regime in the porous and permeable reservoir rocks are in equilibrium with low-permeability rocks and the measured pressure data is used to calibrate the pressure profile. Interestingly, most of the wells drilled in the study area exhibited more or less similar geopressure profiles, where formations above middle Miocene were in hydrostatic pressure regime (0.5 – 0.6 psi/ft), and lower Miocene formation shows steep pressure ramp over 3 psi/ft (Figure-6).

Well-Log Analysis and Depositional Environment

Petrophysical analysis was performed on key-wells to understand the clay-typing (Figures 7 and 8) across the regional mid-Miocene unconformity, where significant increase in illite-trend was observed in the overpressured zones with thorium-potassium cross-plots. Also, a condensed snapshot of Wells-A,B, and C was studied for the petrophysical well-log response across the main unconformity (Figure 9). Significant break in resistivity, neutron-density, and compressional slowness can be observed across the blue arrow that marks the pressure boundary.

The acoustic logs suggested a feeble rotation in the stress regime across the pressure seal (Figure 10); from almost W-E in lower Miocene to NW-SE in middle Miocene. Geological analysis by Arreguin-Lopez et al. (2011) suggested that the middle Miocene formations are actually more confined than the lower Miocene. Also, the middle Miocene shows more slumping features as well. The effect of compressional stresses becomes more apparent moving upwards in the stratigraphic column. In the study area, this upward "increase in confinement" of sand bodies gives rise to the "localized" barriers that in each case may not be traced in all the wells. However, the regional seals are mostly associated with the overbank and passive sedimentation that are present extensively in the study area, encapsulating the intermittent sand bodies and thereby contributing to overpressure.

The borehole image interpretation revealed the variations in the facies assemblages corresponding to the structure and architectural elements of the depositional environment. The middle Miocene bedding shows WNW-ESE strike and SSW dip azimuth in wells A and C. However, the lower Miocene bedding shows a different trend in well-A, where a southeasterly dip azimuth is observed, compared to southwesterly in lower Miocene (Figure 11).

The borehole image logs (Figure-12) also illustrate two distinct types of sand facies for reservoirs. Figure 12A shows around 1-m thick sands (bright yellow units on static image, where gamma-ray log indicates "cleaner" units. This is representative of unconfined setting deposition; which is more prevalent in the lower Miocene. Figure 12B shows thicker sands deposits (bright yellow units on static image, with cleaner gamma-ray response), in a more confined setting (more prevalent in middle Miocene), which is also evident from higher-angle dips picked on the image.
Over the reservoir zone, overpressure tends to accumulate more in the unconfined settings where intercalation of sand/ shale contributes to barrier development.

These units underlain and overlain by regional shale can be sealed off from pressure communication and can contribute to overpressure. Individual well interpretation helps in identification and correlation, or lack of it, for these units across the field. Such models help in understanding the extent of sands and possible barriers that can be expected in such system.

Summary

In the study area, pressure compartments can be clearly observed in pore pressure profiles of drilled wells. The study suggests that compartmentalization commences from lower Miocene formations and pressure gradient varies in that interval from 1psi/ft to over 3psi/ft in the study area. Petrophysical study carried out in these compartments shows increased concentration of illite, which might have been diagenetic product of smectite. Apart from this, stress rotation and changes in log responses have also been observed in middle and lower Miocene formations. This corresponds to a regional unconformity between Middle and Lower Miocene and some local barriers attributed to tectonism and depositional setting. The results of this study can be further integrated with the future wells to better comprehend the pressure barriers and subsurface geological and petrophysical characteristics.

Reference Cited

Arreguín-López, M.A., G. Reyna-Martínez, H. Sánchez-Hernández, A. Escamilla-Herrera, and A. Gutiérrez-Araiza, 2011,Tertiary turbidite systems in the southwestern Gulf of Mexico: Gulf Coast Association of Geological Societies Transactions, v. 61, p. 45–53.

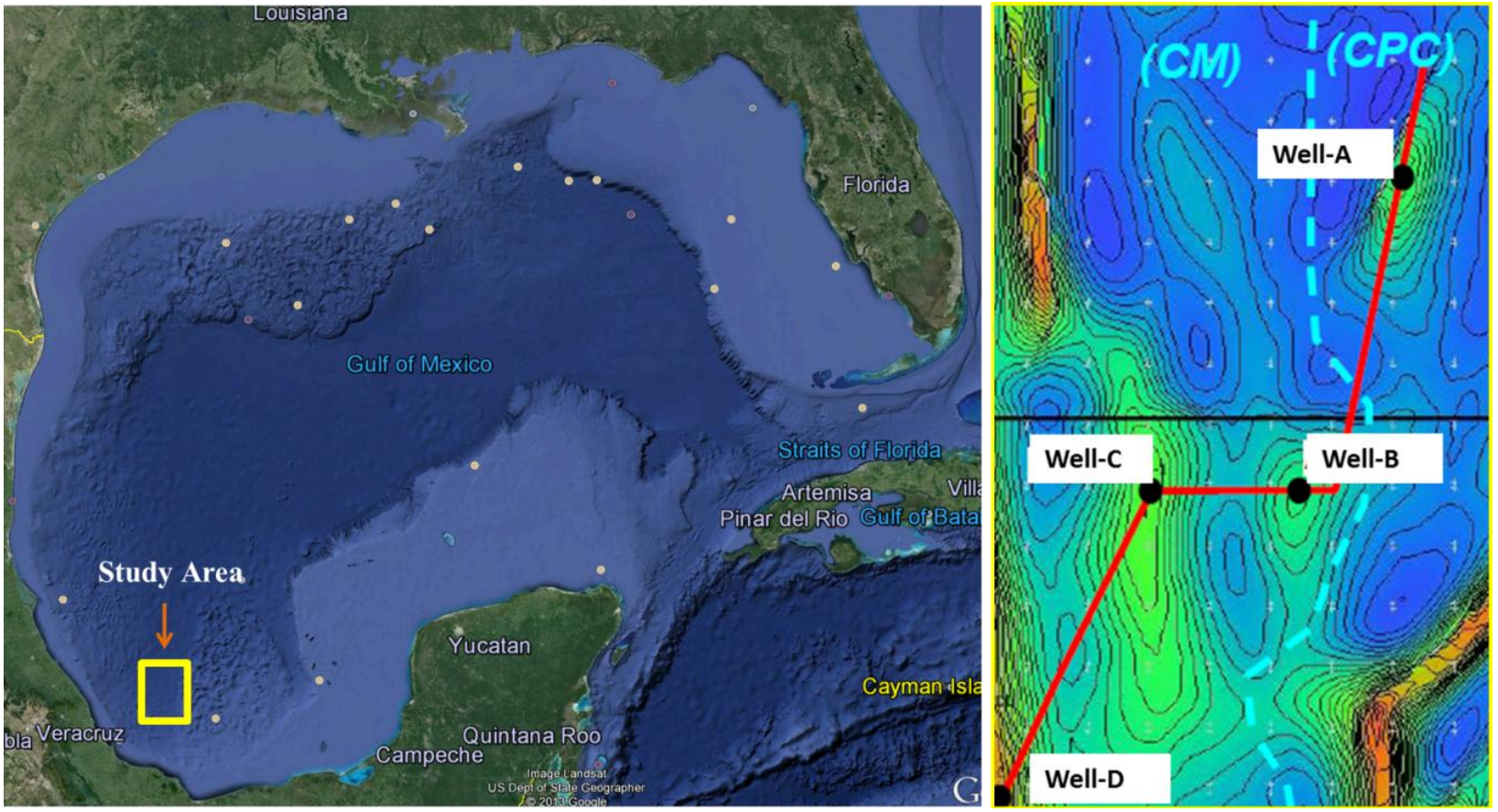

Figure 1. Study area with well locations.

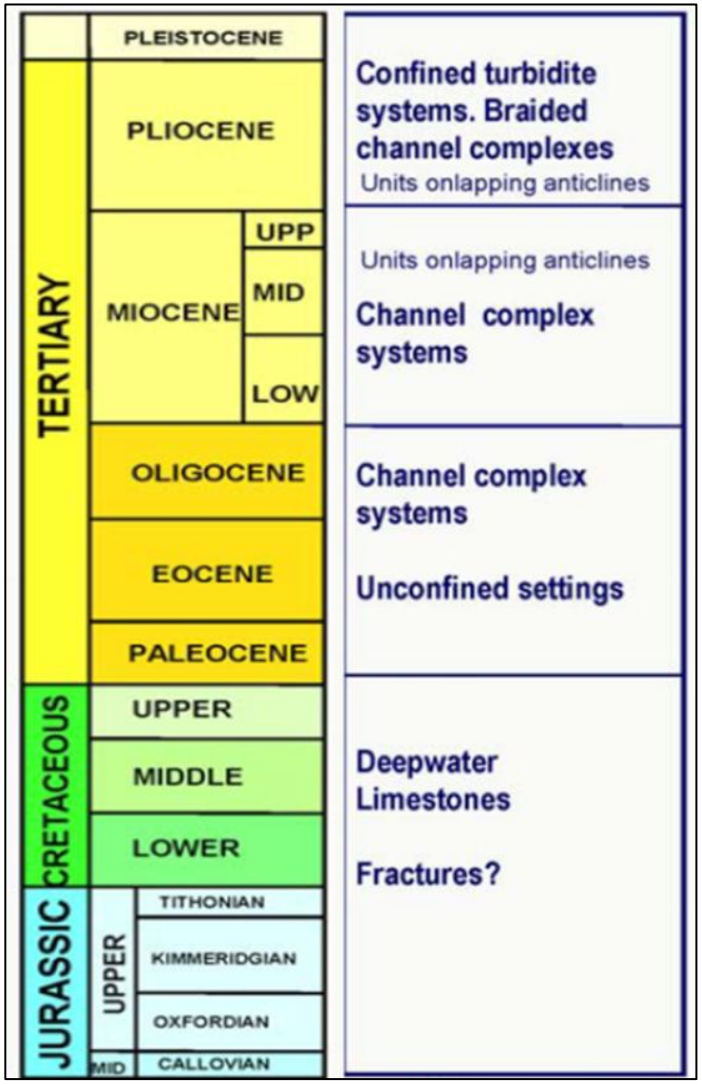

Figure 2. Stratigraphy in the study area (modified after Arreguin-Lopez, 2011).

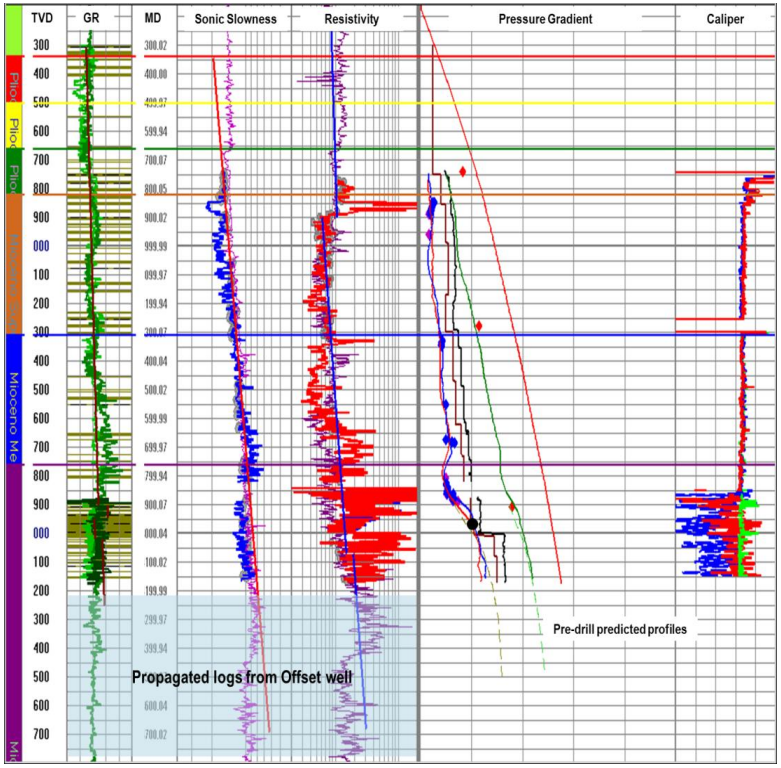

Figure 3. Well-A real-time pressure profile along with LWD logs. Pore pressure profile, calibrated with the measured pressure data down to the upper part of lower Miocene, suggests increasing pore pressure gradient after entering lower Miocene formation. Left to right; Track 1: updated stratigraphic column in the well; Track 2: True vertical depth; Track 3: Gamma Ray from offset well (dark green) and current well (light green); Track 4: Measured depth; Track 5: Compressional slowness from offset well (purple) and current well (blue); Track 6: Resistivity from offset well (purple) and current well (red); Track 7: Pore pressure computed using Eaton's normal compaction trend-line method--Sonic (blue) and Resistivity (red), Mud density (brown) and equivalent circulating density (black) used during drilling, measured pressure data (blue diamonds), leak-off test data (red diamonds), influx pressure (black circle), fracture gradient (solid green), overburden gradient (red), predicted pore pressure (dashed olive) and predicted fracture gradient (dashed green) and Track 8: Caliper (solid red and blue) and density-porosity (dashed blue and red).

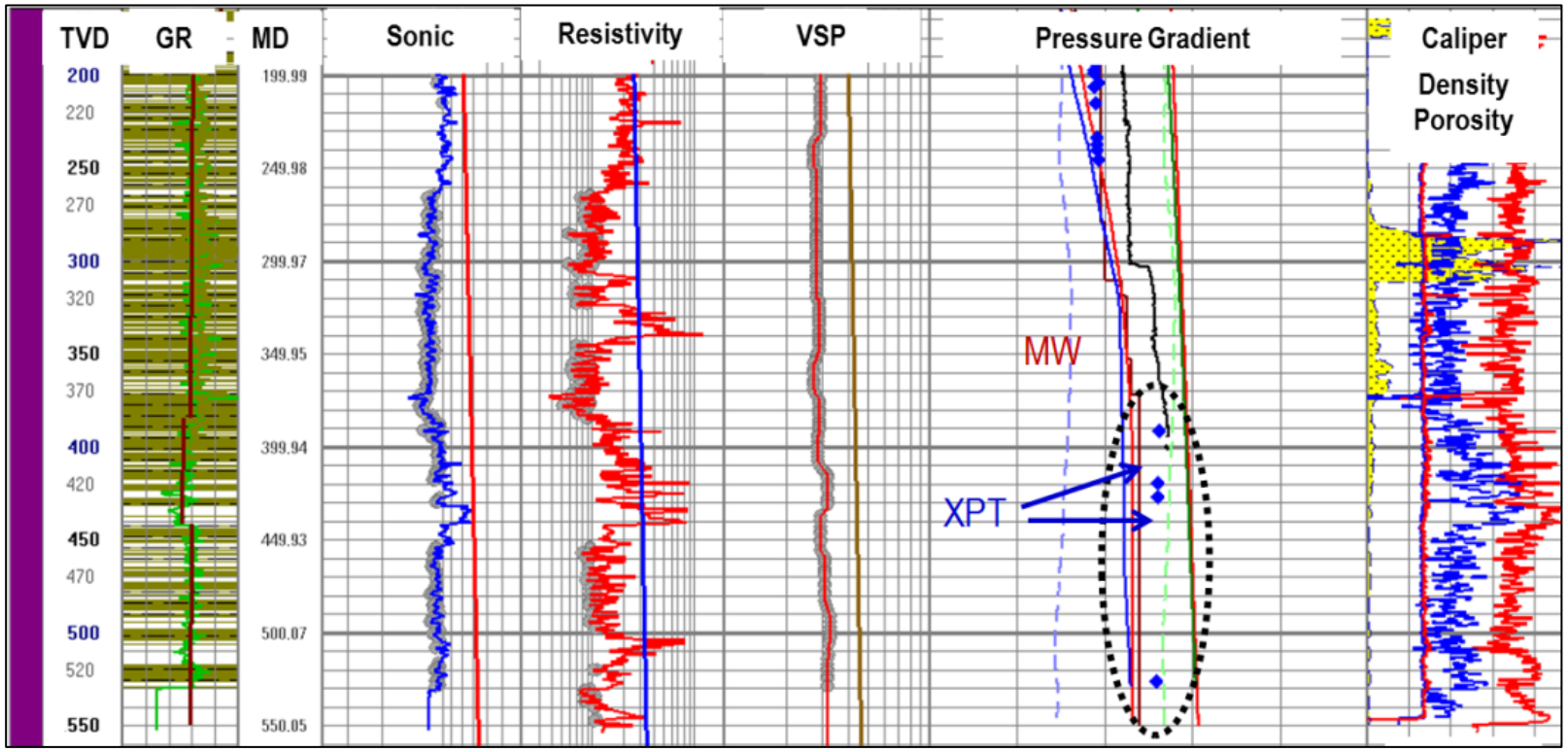

Figure 4. Well-A post-drill calibrated geopressure profile with measured pressure data in lower Miocene formations, increasing geopressure gradient was underestimated in pre-drill and real-time modeling. Left to right; Track 1: Updated stratigraphic column in the well; track 2: True vertical depth; Track 3: Gamma Ray (green); Track 4: Measured depth; Track 5: Compressional sonic slowness (blue); Track 6: Resistivity (red); Track 7: Vertical seismic profile; Track 8: Pore pressure computed using Eaton's normal compaction trend-line method--Sonic (blue) and Resistivity (red), Mud density (brown) and equivalent circulating density (black) used during drilling, measured pressure data (blue diamonds), fracture gradient (solid green), overburden gradient (red), predicted pore pressure (dashed blue) and predicted fracture gradient (dashed green); Track 9: Caliper (solid red and blue), density-porosity (dashed blue and red) and total gas readings during drilling (shaded yellow region).

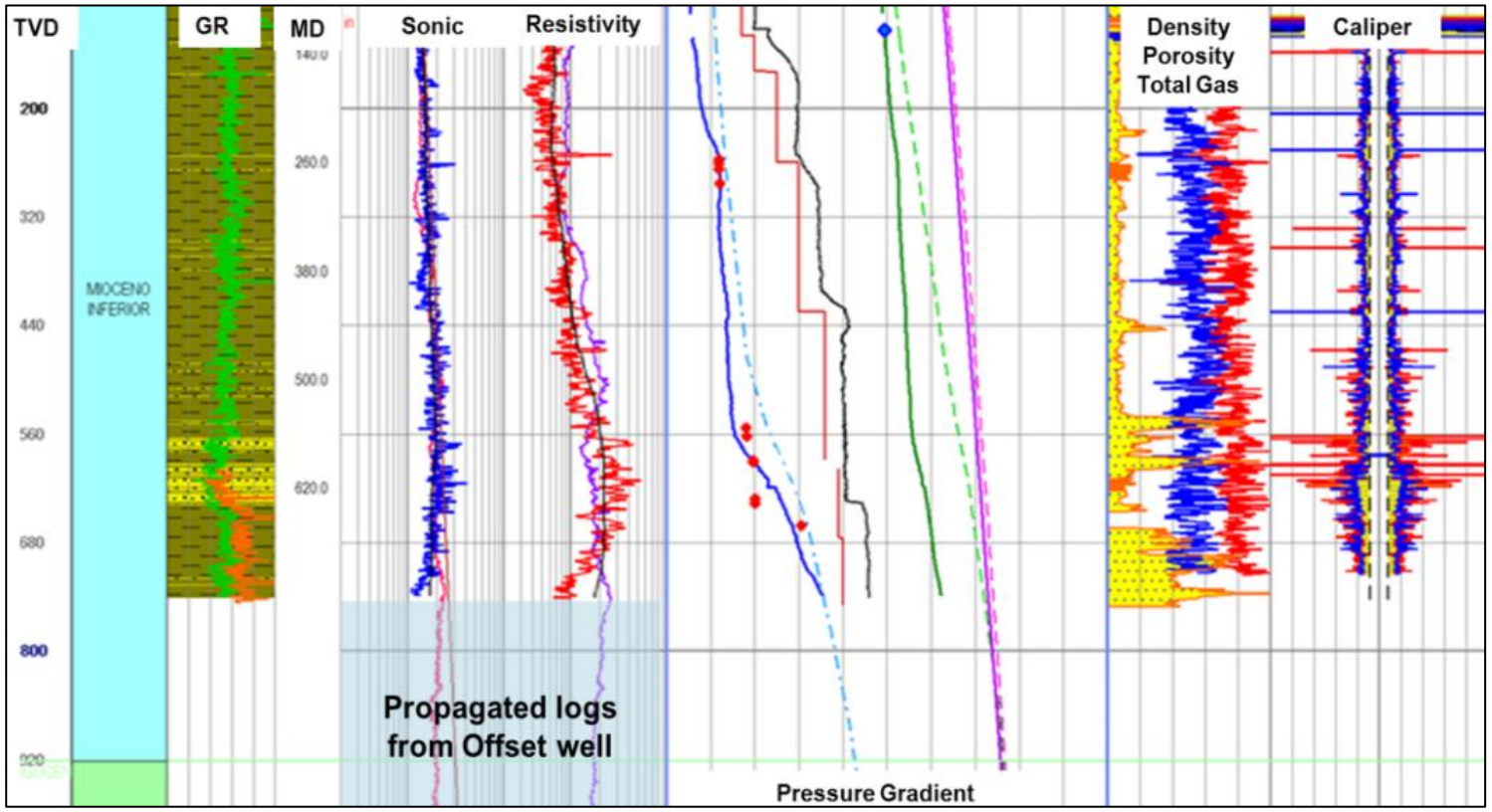

Figure 5. Post-drill calibrated geopressure profile with pressure data collected in lower Miocene formations of well-B. Left to right; Track 1: True vertical depth; Track 2: updated stratigraphic column in the well; Track 3: Gamma Ray (green); Track 4: Measured depth; Track 5: Compressional slowness from offset well (gray) and current well (blue); Track 6: Resistivity from offset well (gray), current well (red); Track 7: Pore pressure computed using Eaton's normal compaction trend-line method--Sonic (blue), Mud density (brown) and equivalent circulating density (black) used during drilling, measured pressure data (blue diamonds), leak-off test data (blue diamond), fracture gradient (solid green), overburden gradient (pink), predicted pore pressure (dashed blue), predicted fracture gradient (dashed green) and predicted overburden (dashed pink); Track 8: Density-porosity (red and blue) and total gas readings during drilling (shaded yellow region) and Track 9: Caliper (solid red and blue) along with bit size in the section.

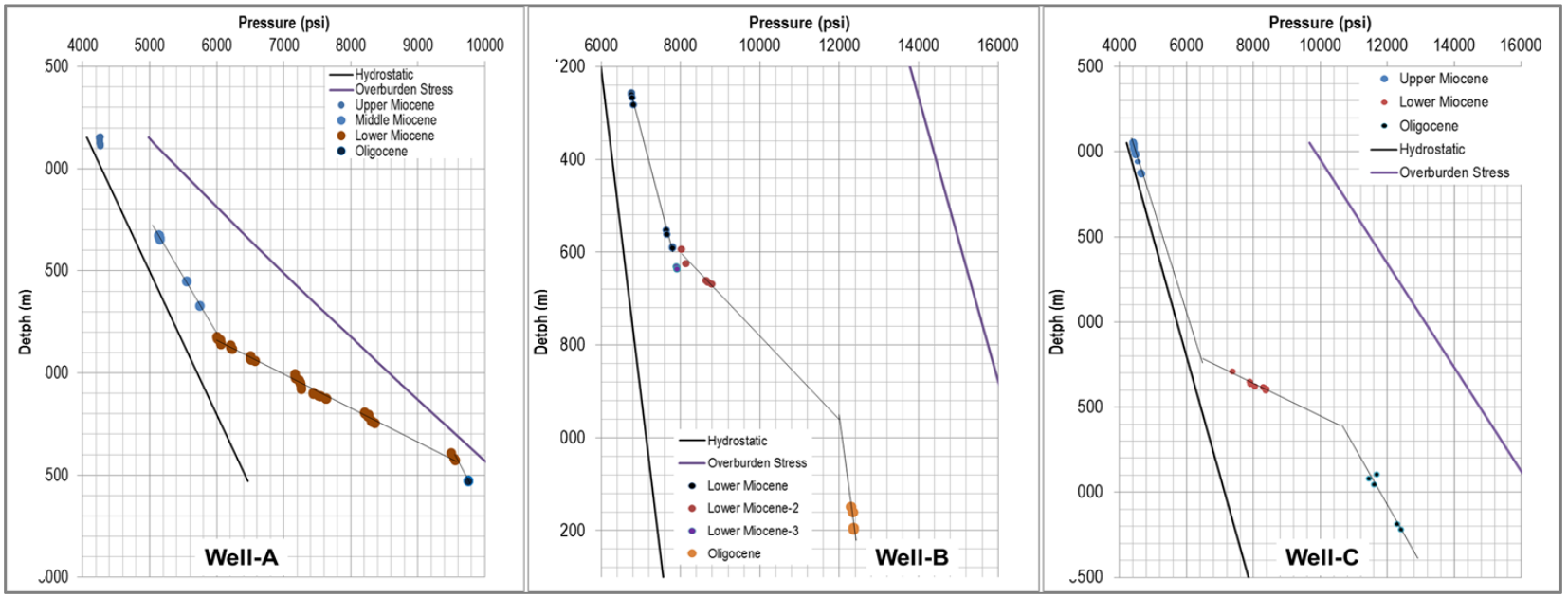

Figure 6. Measured pressure data collected and color-coded to differentiate in various formations in the wells drilled. Upper and middle Miocene formations show near hydrostatic pressure trend, whereas steep pressure ramp can be observed in lower Miocene formation.

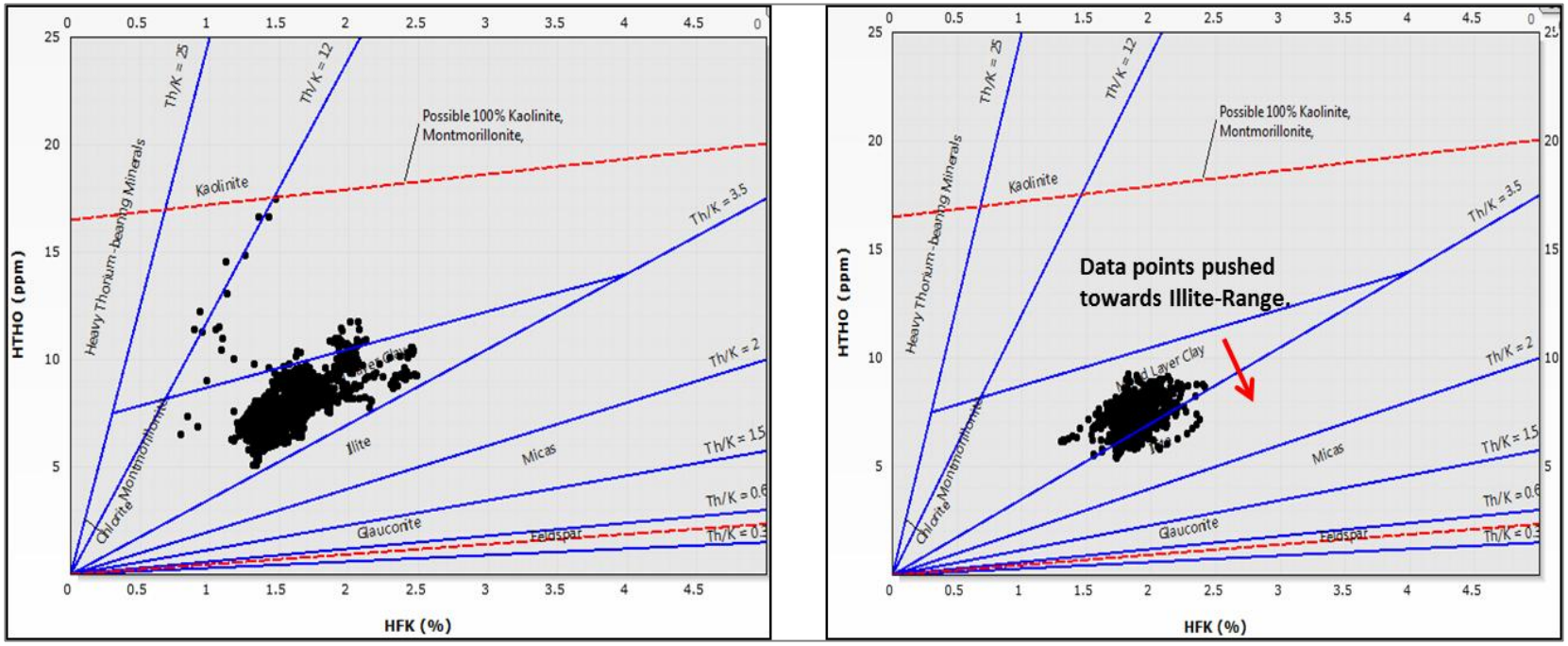

Figure 7. Clay-typing in well-A across the unconformity; more illite in overpressured zone as shown by the red arrow where data points tend towards illite zone in the cross-plot.

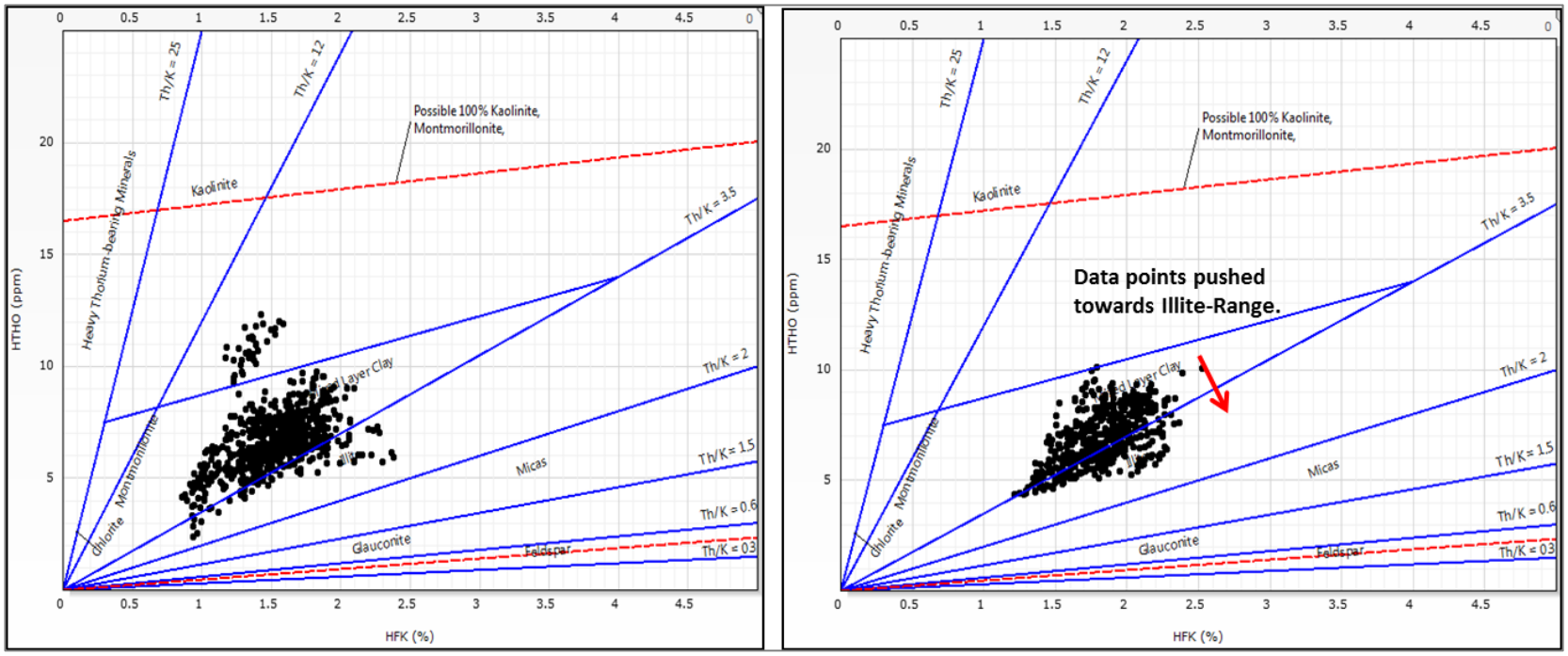

Figure 8. Clay-typing in well-C across the unconformity; more illite in overpressured zone as shown by the red arrow where data points tend towards illite zone in the cross-plot.

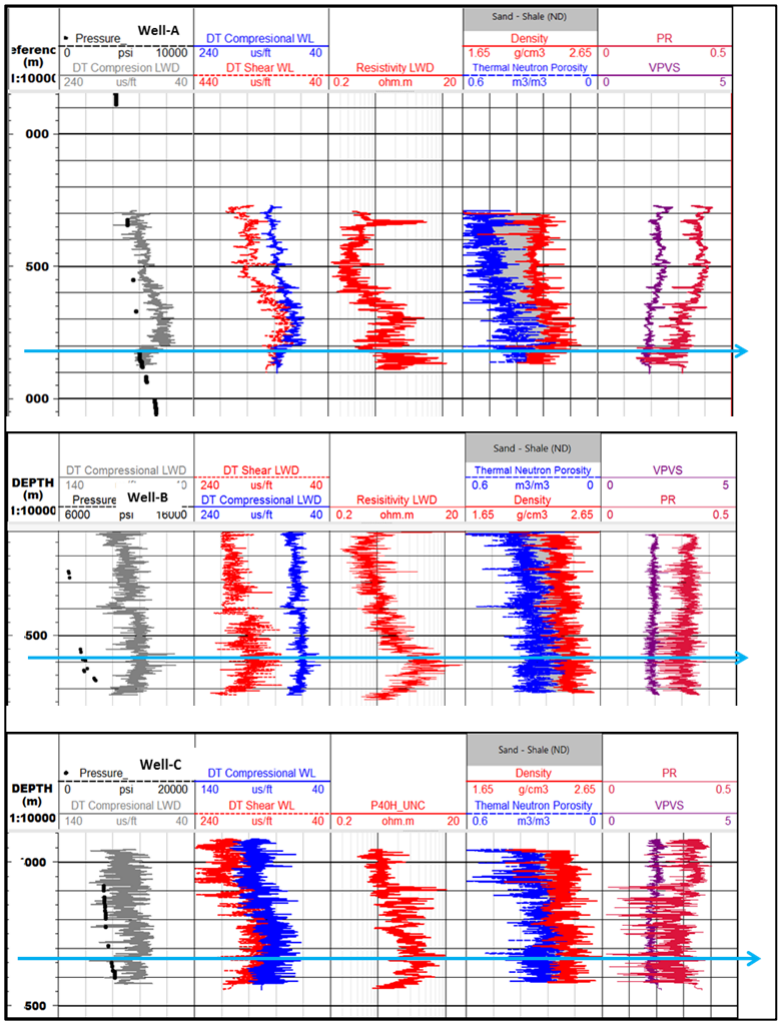

Figure 9. Some petrophysical logs across the major pressure boundary (shown with blue arrow), showing changed petrophysical properties across the seal in Wells-A, -B, and -C, respectively. The black dots in the second track show the pressure profile from formation testers.

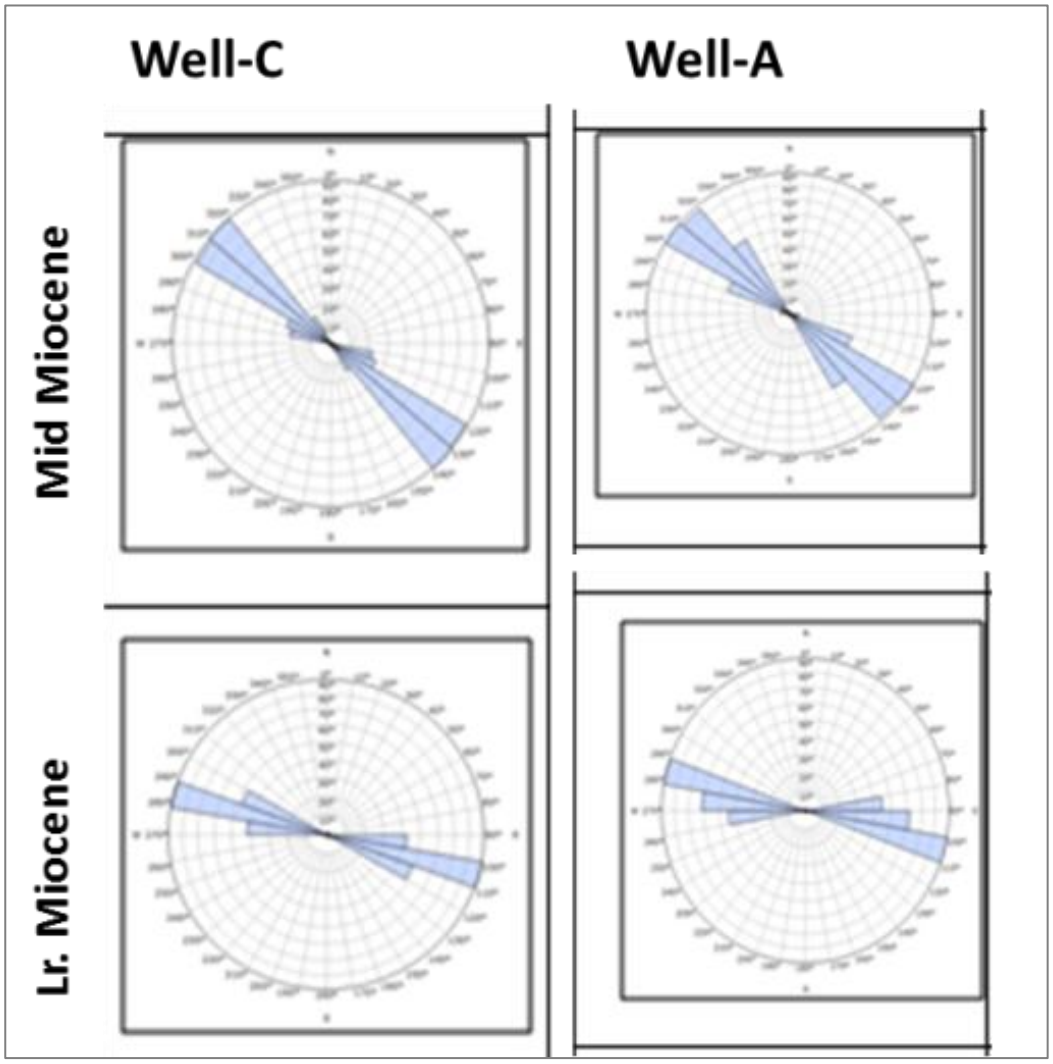

Figure 10. Maximum horizontal stress direction in study wells from acoustic logs.

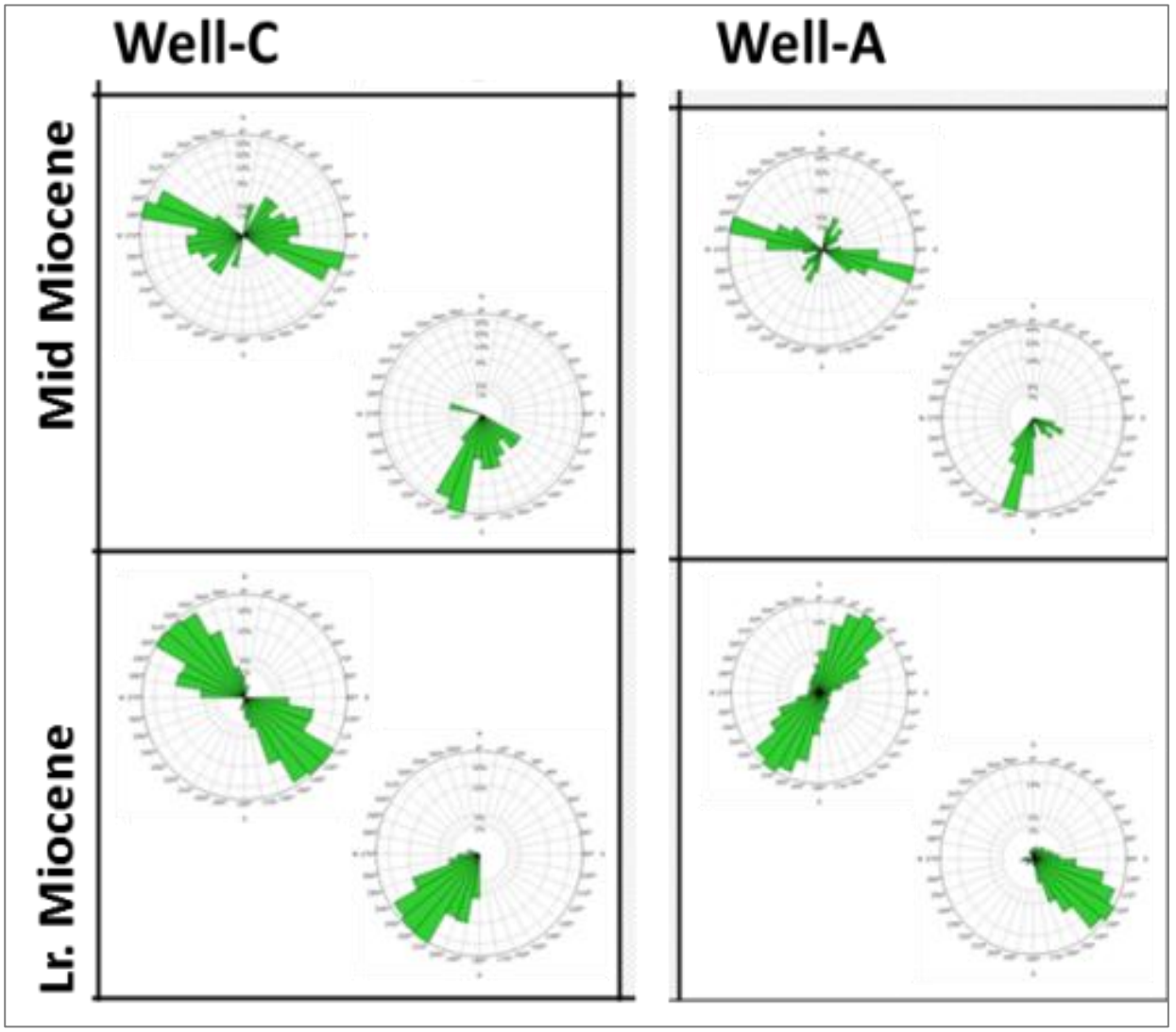

Figure 11. Bedding dip and strike (azimuth) in 2 key wells.

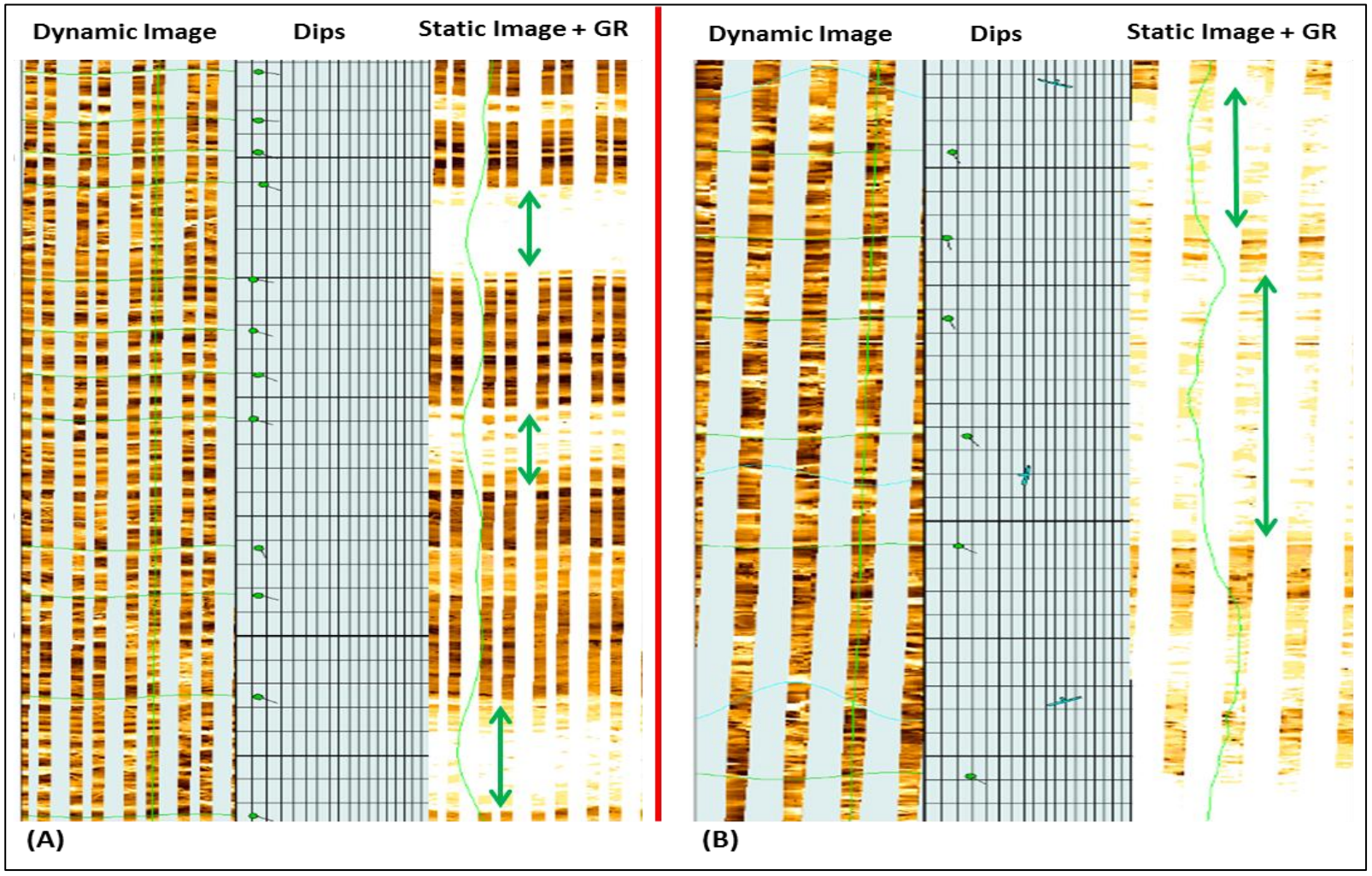

Figure 12. Examples of borehole image showing sands (bright yellow in static image) in unconfined setting (A) and confined setting (B).